Contribution of a mutational bias in hepatitis C virus replication to the genetic barrier in the development of drug resistance

Megan H. Powdrill[a,1], Egor P. Tchesnokov[a,1], Robert A. Kozak[b], Rodney S. Russell[c], Ross Martin[d], Evguenia S. Svarovskaia[d], Hongmei Mo[d], Roger D. Kouyos[e], and Matthias Götte[a,b,2]

[a]Department of Microbiology and Immunology, McGill University, 3775 University, Montreal, QC, Canada H3A 2B4; [b]Department of Biochemistry, McGill University, 3655 Sir William Osler Promenade, Montreal, QC, Canada H3A 1A3; [c]Division of BioMedical Sciences, Memorial University of Newfoundland, 300 Prince Philip Drive, St. John's, NF, Canada A1B 3V6; [d]Gilead Sciences, Inc., 333 Lakeside Drive, Foster City, CA 94404; and [e]Department of Ecology and Evolutionary Biology, Princeton University, Guyot Hall, Princeton, NJ 08544

Edited by* Charles M. Rice, The Rockefeller University, New York, NY, and approved September 29, 2011 (received for review April 11, 2011)

The development of resistance to direct-acting antivirals (DAAs) targeting the hepatitis C virus (HCV) can compromise therapy. However, mechanisms that determine prevalence and frequency of resistance-conferring mutations remain elusive. Here, we studied the fidelity of the HCV RNA-dependent RNA polymerase NS5B in an attempt to link the efficiency of mismatch formation with genotypic changes observed in vivo. Enzyme kinetic measurements revealed unexpectedly high error rates (approximately 10^{-3} per site) for G:U/U:G mismatches. The strong preference for G:U/U:G mismatches over all other mistakes correlates with a mutational bias in favor of transitions over transversions. Deep sequencing of HCV RNA samples isolated from 20 treatment-naïve patients revealed an approximately 75-fold difference in frequencies of the two classes of mutations. A stochastic model based on these results suggests that the bias toward transitions can also affect the selection of resistance-conferring mutations. Collectively, the data provide strong evidence to suggest that the nature of the nucleotide change can contribute to the genetic barrier in the development of resistance to DAAs.

Approximately 170 million people worldwide are infected with hepatitis C virus (HCV) (1). Chronically infected individuals are at risk of developing severe liver disease, including cirrhosis and hepatocellular carcinoma (2). Although the infection can be cured with a combination of interferon-α and ribavirin, severe side effects and complicated treatment schedules can compromise therapy (3). Moreover, the response is particularly poor in patients infected with HCV genotype 1, which is the most prevalent genotype in North America and Europe (4).

Several direct-acting antivirals (DAAs) targeting important viral and host factors are currently undergoing clinical evaluation. Drugs acting against the viral NS5B RNA-dependent RNA polymerase (RdRp) or NS3 protease are in advanced clinical trials, with the protease inhibitors (PIs) telaprevir and boceprevir recently gaining FDA approval. Combining interferon-α and ribavirin with either PI can produce increases in sustained virological response when compared with the combination of interferon-α and ribavirin without PI (5, 6). However, the emergence of resistance-conferring mutations can lead to treatment failure (7). Like other RNA viruses, HCV shows quasispecies-like characteristics (8). Accordingly, resistant variants are selected from a genetically highly diverse population. Resistance to PIs is rapidly selected in cell-based replicon systems and in vivo (9). Similar observations have been made with the various classes of nonnucleoside analogue inhibitors (NNIs) of NS5B (9). Moreover, mutations that decrease susceptibility to highly potent inhibitors of the RNA binding protein NS5A also emerge rapidly in the replicon system (10). In contrast, the barrier to the development of resistance to nucleoside analogue inhibitors (NIs) appears to be significantly higher. The 2′-C-methylated NIs were shown to select in vitro for S282T in NS5B (11). RG7128, the prodrug of PSI-6130, is currently the most advanced NI; however, the S282T mutation has not been identified in clinical samples of patients treated with this drug (12). Inhibitors of the host factor cyclophilin provide another example for a high barrier to the emergence of resistance. Debio 025 (alisporivir) and other structurally distinct cyclophilin inhibitors were shown to select for D320E in NS5A. Like S282T, this mutation emerges late in replicon-based selection experiments, and confers only low levels of resistance to the drug (13, 14).

Parameters that determine the outcome of a selection process are multifactorial and include the fitness of the mutant variant, the level of resistance that the specific mutation confers, and its availability within a given viral population. The HCV-associated RdRp is often described as an error-prone enzyme that is the source of genetic diversity, and, in turn, availability of mutant viruses. However, the fidelity of HCV NS5B remains to be determined. Here, we employed biochemical techniques to measure error rates for all possible nucleotide mismatches. Our data reveal a strong preference for formation of G:U and U:G mismatches. These findings correlate with deep sequencing analyses of HCV samples from treatment-naïve patients that show higher frequencies of transitions over transversions within the diversity of their viral quasispecies. A stochastic model supports our conclusion that the genetic barrier associated with the selection of resistant HCV variants is higher for transversions.

Results and Discussion

Fidelity of HCV NS5B. NS5B is able to initiate RNA synthesis de novo; i.e., in the absence of a primer (15). The initiation reaction is fragile, and the complex composed of NS5B and RNA template dissociates frequently (16). The transition to the highly processive elongation mode is evident after incorporation of two to four nucleotides. It is, therefore, reasonable to assume that mutations emerging in the coding region for structural and nonstructural proteins are generated in the context of elongation complexes. To mimic this stage of RNA synthesis, we designed short RNA templates that allowed us to stall NS5B at defined positions through the use of limited nucleoside triphosphate (NTP) pools (Fig. 1*A*). The efficiency of incorporation of correct versus incorrect nucleotides is then monitored at the next tem-

Author contributions: M.H.P., E.P.T., E.S.S., R.D.K., and M.G. designed research; M.H.P., E.P.T., and R.D.K. performed research; M.H.P., E.P.T., R.A.K., R.S.R., R.M., E.S.S., R.D.K., and M.G. analyzed data; and M.H.P., E.S.S., H.M., R.D.K., and M.G. wrote the paper.

The authors declare no conflict of interest.

*This Direct Submission article had a prearranged editor.

Freely available online through the PNAS open access option.

[1]M.H.P and E.P.T. contributed equally to this work.

[2]To whom correspondence should be addressed. E-mail: matthias.gotte@mcgill.ca.

This article contains supporting information online at www.pnas.org/lookup/suppl/doi:10.1073/pnas.1105797108/-/DCSupplemental.

BIOCHEMISTRY

plate position (Fig. 1*B*). Kinetic parameters k_{pol} and K_d are direct measures for the maximum rate of the reaction and affinity to the nucleotide substrate, respectively (Fig. 1 *C* and *D*). The efficiency of nucleotide incorporation is defined as the ratio of k_{pol}/K_d, and the error rate per site can be expressed as the ratio of $(k_{pol}/K_d)_{\text{incorrect nucleotide}}/(k_{pol}/K_d)_{\text{correct nucleotide}} + (k_{pol}/K_d)_{\text{incorrect nucleotide}}$. Incorporation of a "correct" nucleotide results in canonical Watson–Crick base pairing, whereas incorporation of an "incorrect" nucleotide results in mismatch formation.

We found that K_d values for incorporation of correct nucleotides range between 110–490 μM, and k_{pol} values range between 10 and 27 s^{-1} (Table 1). The values are comparable with kinetic parameters determined for other related viral RdRps (17, 18). For mismatch incorporations, we observe both decreases in k_{pol} and increases in K_d values for each of the 12 possible combinations. However, the magnitude of these changes depends profoundly on the nature of the mismatch. The efficiency of formation of G:U and U:G mismatches is markedly higher when compared with all other combinations. For G:U mismatches we measured error rates/per site of 3.2×10^{-3}, and 8.7×10^{-3} for the complementary U:G mismatch. Error rates for all other combinations were markedly lower and vary between 9.2×10^{-5} (A:C) and 1.4×10^{-6} (A:G). Similar incorporation efficiencies were measured with an unrelated sequence, which demonstrates a general trend (Tables S1 and S2).

Additional kinetic measurements revealed that the extension of a mismatch is at least three orders of magnitude more efficient when compared to the related mismatch incorporation event (Fig. S1*A* and *B*). These data are in agreement with measurements on other polymerases, and show that incorporation of the incorrect nucleotide is the rate-limiting step (19). In order to translate error rates per site into error rates per genome replication, we considered, therefore, only rates of incorporation, along with differences in the base composition of the HCV genome. HCV shows a high GC-content: A(1910), C(2883), G(2733), and U(2079) for the reference isolate Con 1 (genotype 1b). For non-G:U/U:G mismatches we calculate error rates between 2.7×10^{-3} (A:G) and 2.0×10^{-1} (C:U) mistakes per genome replication. In contrast, for G:U and U:G mismatches we calculate 8.7 and 18 mistakes, respectively. Thus, our data suggest a 6,500-fold difference between the two extremes A:G and U:G.

Overall, the error rates for non-G:U/U:G mismatches are at the lower end of previous estimates associated with (+)-strand RNA viruses, whereas the error rates for G:U and U:G mismatches are at the high end (20, 21). A point of caution is that biochemical measurements are restricted to a few sites, and error rates per genome replication can only be extrapolated and not accurately determined from this data. Moreover, effective concentrations and variations of intracellularly available nucleotide pools at the site of viral replication are unknown. Discrepancies between error rates measured in biochemical versus cell culture experiments have been reported for HIV (22). Up to 20-fold higher rates are commonly measured with purified HIV-1 RT. The high rates for G:U/U:G mismatches introduced by HCV NS5B may likewise overestimate the error frequency associated with viral replication. However, the difference in relative efficiencies with which the various mismatches are generated is striking and raises the question of whether the preferred formation of

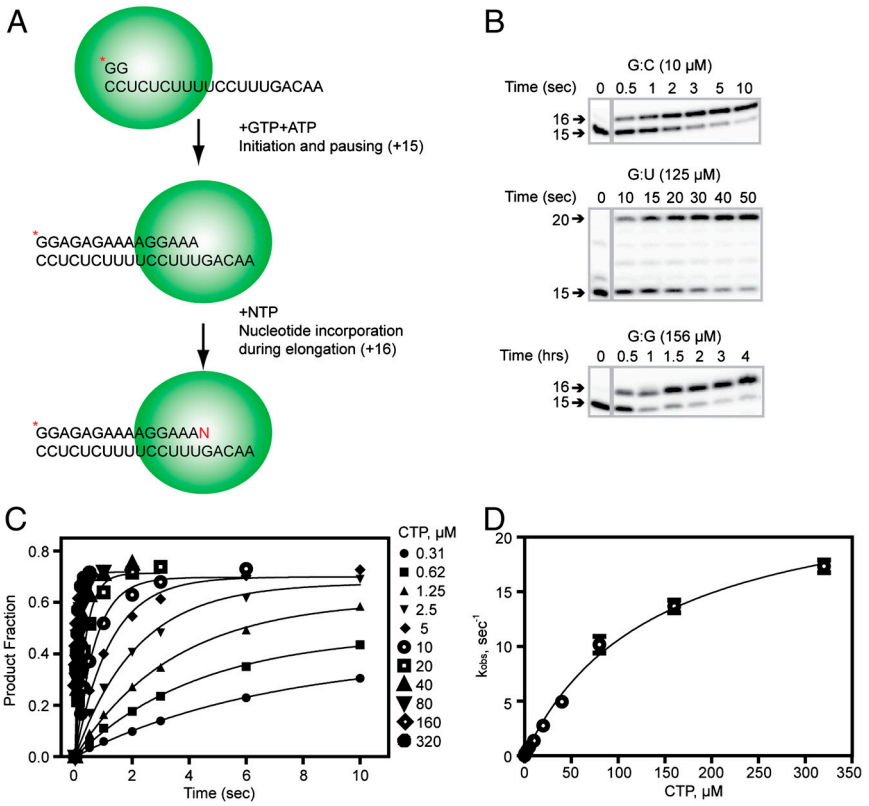

Fig. 1. Pre-steady-state kinetics of single nucleotide incorporations. The figure shows examples of NTP incorporation opposite template G to illustrate the experimental procedure and data analysis. (*A*) Extension of a radio-labeled dinucleotide primer is limited to position +15. Correct or mismatched (incorrect) nucleotides are then added at increasing concentrations. (*B*) Gel-based analysis show the extended primer at position +15, and increasing product formation at position +16 or +20, depending on the requirements for NTPs. (*C*) Time-dependent changes in product formation for various concentrations of CTP. The data points were fit to a single exponential curve to obtain observed incorporation rate constants (k_{obs}). (*D*) Rates were then plotted against nucleotide concentration and fit to the hyperbolic equation $Y = (k_{pol} * X)/(K_d + X)$ to obtain maximum rate of incorporation (k_{pol}) and the equilibrium dissociation constant (K_d). Error bars represent the standard deviation determined from three independent experiments.

Table 1. Kinetic parameters of correct or incorrect nucleotide incorporation by HCV NS5B

Template base	NTP	K_d, μM	k_{pol}, s^{-1}	k_{pol}/K_d, $\mu M^{-1} s^{-1}$	Error rate/site	Error rate/genome
A	UTP	$4.9 \times 10^2 \pm 1.1 \times 10^2$	$2.7 \times 10^1 \pm 3.5 \times 10^0$	5.6×10^{-2}	—	
	ATP	$5.0 \times 10^3 \pm 3.8 \times 10^2$	$5.0 \times 10^{-3} \pm 2.9 \times 10^{-4}$	1.0×10^{-6}	1.8×10^{-5}	3.4×10^{-2}
	CTP	$2.6 \times 10^3 \pm 5.8 \times 10^2$	$1.4 \times 10^{-2} \pm 1.9 \times 10^{-3}$	5.1×10^{-6}	9.2×10^{-5}	1.8×10^{-1}
	GTP	$1.7 \times 10^3 \pm 7.9 \times 10^2$	$1.4 \times 10^{-4} \pm 2.7 \times 10^{-5}$	8.0×10^{-8}	1.4×10^{-6}	2.7×10^{-3}
C	GTP	$1.1 \times 10^2 \pm 7.8 \times 10^0$	$9.6 \times 10^0 \pm 2.6 \times 10^{-1}$	9.0×10^{-2}	—	
	ATP	$7.8 \times 10^3 \pm 3.9 \times 10^3$	$1.6 \times 10^{-3} \pm 5.6 \times 10^{-4}$	2.1×10^{-7}	2.3×10^{-6}	6.6×10^{-3}
	CTP	$4.9 \times 10^3 \pm 1.6 \times 10^3$	$1.0 \times 10^{-2} \pm 2.1 \times 10^{-3}$	2.1×10^{-6}	2.4×10^{-5}	6.8×10^{-2}
	UTP	$6.2 \times 10^3 \pm 2.4 \times 10^2$	$3.8 \times 10^{-2} \pm 1.2 \times 10^{-3}$	6.2×10^{-6}	6.9×10^{-5}	2.0×10^{-1}
G	CTP	$1.4 \times 10^2 \pm 1.0 \times 10^1$	$2.0 \times 10^1 \pm 6.7 \times 10^{-1}$	1.4×10^{-1}	—	
	ATP	$2.7 \times 10^3 \pm 2.7 \times 10^2$	$6.2 \times 10^{-3} \pm 4.0 \times 10^{-4}$	2.3×10^{-6}	1.6×10^{-5}	4.4×10^{-2}
	GTP	$4.6 \times 10^2 \pm 1.4 \times 10^2$	$1.4 \times 10^{-3} \pm 1.5 \times 10^{-4}$	3.1×10^{-6}	2.1×10^{-5}	5.8×10^{-2}
	UTP	$7.5 \times 10^2 \pm 1.4 \times 10^2$	$3.5 \times 10^{-1} \pm 3.6 \times 10^{-2}$	4.6×10^{-4}	3.2×10^{-3}	8.7×10^0
U	ATP	$4.5 \times 10^2 \pm 8.3 \times 10^1$	$1.6 \times 10^1 \pm 1.7 \times 10^0$	3.5×10^{-2}	ref	
	CTP	$1.7 \times 10^3 \pm 4.2 \times 10^2$	$9.7 \times 10^{-4} \pm 1.3 \times 10^{-4}$	5.8×10^{-7}	1.7×10^{-5}	3.4×10^{-2}
	GTP	$1.3 \times 10^3 \pm 1.9 \times 10^2$	$3.9 \times 10^{-1} \pm 3.6 \times 10^{-2}$	3.0×10^{-4}	8.7×10^{-3}	1.8×10^1
	UTP	$2.3 \times 10^3 \pm 3.9 \times 10^2$	$1.3 \times 10^{-3} \pm 1.1 \times 10^{-4}$	5.8×10^{-7}	1.7×10^{-5}	3.5×10^{-2}

Error rate per site = $(k_{pol}/K_d)_i/(k_{pol}/K_d)_i + (k_{pol}/K_d)_c$.
Error rate per genome = error rate per site × frequency of corresponding base in genome.

G:U/U:G mispairs correlates with a mutational bias at the level of viral replication in vivo.

Mutational Bias in HCV Replication. To address this question, we performed deep sequencing analysis of HCV RNA samples derived from 20 HCV-infected, treatment-naïve individuals. In efforts to reduce complexity, this analysis was restricted to the NS3 region of the HCV genome. Table S3 summarizes the data and shows the total number of mutations for each possible combination. The average number of base-read positions that were sampled per patient was 781,844 with an average of 7,385 base changes per patient, which translates to an observed error rate of 9.4×10^{-3}. Most importantly, HCV viral variant subpopulations were represented mainly by transitions (Fig. 2). The median frequency of transitions (1.35×10^{-3}), normalized to the total number of base-read positions, is approximately 75-fold higher as compared to the median frequency of transversions (1.75×10^{-5}) (Fig. 2 and Table S3). Similar data were obtained from sequences amplified from passaged replicon cells. The assay background levels of substitutions for plasmid controls were significantly lower with only 67 mutants observed among 3,764,286 tested base-read positions. The reverse transcription step is associated with an error rate of 1.6×10^{-5} (displaying a 5-fold preference for transitions over transversions) (23), which is also significantly lower when compared with our observed error rates of 9.4×10^{-3} per patient.

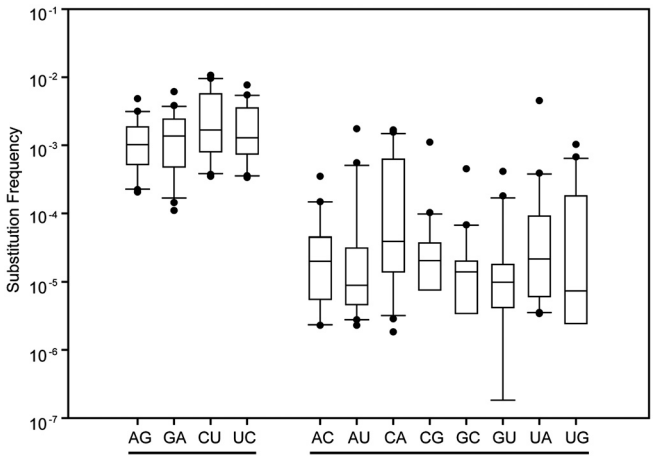

Fig. 2. Deep sequencing analysis of transition and transversion frequencies in vivo. The box plot shows the medians, upper and lower quartile of mutation frequencies observed in samples of 20 HCV-infected, treatment-naïve individuals. Mutations are grouped in nucleotide transitions (e.g., AG: A to G) and transversions (e.g., AC: A to C). Mutation frequencies are normalized to total base-read positions. Outliers are shown as black dots. Note that values associated with the few outliers are commonly driven by relatively high frequencies of only one or two transversions (Table S3).

The pronounced bias toward transitions correlates with our biochemical data. A to G transitions can be generated via A:C or U:G mismatches, provided that mismatches can occur during both (−)- and (+)-strand RNA synthesis (Fig. S2*A*). In this case we would expect, based on our kinetics studies, that the genetic pathway via U:G mismatches during (+)-strand RNA synthesis is favored. Conversely, U to C transitions can be generated through U:G [(−)-strand] or A:C [(+)-strand] mismatches (Fig. S2*B*), which suggests that in this case the error is more frequently made during (−)-strand RNA synthesis. C to U and G to A transitions can also be generated through either C:A or G:U mismatches, or through G:U or C:A mismatches, respectively (Fig. S2 *C* and *D*). Thus, the four transitions can all be generated through U:G or G:U mismatches that are easily formed in cell-free, biochemical assays. In contrast, each of the eight transversions are generated through non-U:G/G:U mismatches that are more difficult to form.

Evidence for the existence of a mutational bias toward transitions is also apparent when HCV evolution is monitored in replicons and in chimpanzees followed by common population sequencing (24, 25), although the number of mutations observed is several orders of magnitude lower when compared with our deep sequencing approach. Other studies have identified amino acid substitutions arising during replication of HCV replicons or infectious viruses (Fig. S3*A* and *B*). Some of the nonsynonymous mutations arising during replication have been confirmed as cell culture adaptive mutations that confer a certain replication advantage over the original HCV variant. The vast majority of amino acid substitutions that have been reported in this context are likewise generated via transitions. Thus, the mutational bias may also be a relevant factor in the selection of drug resistance-conferring mutations. A table comprising all amino acid substitutions generated through single nucleotide changes was created to assess which mutations can be generated via transitions and/or transversions (Fig. S4).

Definition of the Genetic Barrier. Each of the different classes of DAAs that are currently under clinical investigation can select for specific resistance-conferring mutations (7). However, prevalence and frequency of resistance-conferring mutations can depend on the nature of the particular change at the nucleotide and amino acid levels. The "genetic" barrier to the development

BIOCHEMISTRY

of resistance, often defined as the number of nucleotide changes, is likely to be an important parameter in this regard. The PI-associated R155K mutation in NS3 requires a single nucleotide change in genotype 1a (AGG AAG), whereas two changes are required in the context of genotype 1b (CGG AAG) (Fig. S5*A*). R155K is rarely observed in patients infected with genotype 1b, and it is widely accepted that the two required nucleotide changes pose a higher genetic barrier (26). However, based on our data, it is conceivable that the nature of the nucleotide change can also contribute to the genetic barrier. The AGG to AAG change associated with genotype 1a involves a single transition (G to A), whereas the CGG to AAG change associated with genotype 1b involves a transition (G to A) and a transversion (C to A).

Barrier of a Potent Drug Regimen. Rong et al. have recently developed a mathematical model that considers the dynamics of HCV replication and virus production, and calculated that a potent drug regimen requires a barrier of four or more mutations (27). A key assumption of this model is a constant, mean error rate of 10^{-5} per site. Here, we extended this model and assessed the impact of variable mutation rates on the evolution of resistance. We specifically asked whether the barrier of four mutations can be lower depending on the specific mutational pattern, and considered different theoretical scenarios: drug regimens associated with three (Fig. 3), and, for comparative purposes, with four (Fig. S6) different mutations that are generated through generic, single nucleotide transitions and/or transversions. For three transitions, resistance develops at transition rates $<5\times10^{-5}$ (Fig. 3*A*), which is much lower than our actual measurements for G:U/U:G mismatches ($>10^{-3}$). Thus, the development of resistance is highly likely under these circumstances, even in the presence of fitness deficits. Of note, Rong and colleagues specifically analyzed the rapid emergence of telaprevir-associated mutations V36A/M and A156V/T in clinical trials, and these mutations can all be generated through transitions (27). Thus, we next analyzed the effect of an increase in the number of transversions in our stochastic model (Fig. 3 *B*, *C*, and *D*). The data show that the probability of resistance development is gradually decreased, if we consider a 50-fold difference between transitions and transversion frequencies. This value is a conservative estimate derived from our deep sequencing analysis. For the extreme case of three transversions, resistance may not develop at transversion rates $<10^{-5}$. Considering that our measured mutation rates for non-G:U/U:G mismatches vary between 1.4×10^{-6} and 9.2×10^{-5}, it is conceivable that a barrier of three transversions can be sufficient for a potent regimen. The mutation rate required to develop resistance is further increased if a substantial diminution in fitness is considered at the same time. At a fitness cost of 20% per mutation, resistance may not develop at mutation rates $<10^{-4}$, which is higher than our measured rates for transversions. Together, these findings provide strong evidence to suggest that not only the number, but also the nature of the nucleotide change can contribute to the genetic barrier in the development of resistance.

The Mutational Bias and Resistance to DAAs. With the large number of DAAs currently in clinical trials, it will be of interest to study whether certain compounds can be combined to minimize the risk of selecting mutations generated through transitions. PIs were shown to select for a variety of different amino acid changes in NS3. A broad spectrum of selected amino acids is often observed at the same position, including signature mutations R155K/T/Q, A156S/T/V/G, and D168G/A/V/T/H/Y/E (28). The variety of possible amino acid changes at a single position increases opportunities for transitions to occur. For each of these positions, there is at least one amino acid change that can be generated through a transition (Fig. S5 *A*, *B*, and *C*). The spectrum of mutations associated with nonnucleoside NS5B inhibitors (NNIs) and NS5A inhibitors are likewise broad. Signature mutations including M423I (NNI site 1), P495V (NNI site 2), M414T (NNI site 3), C316Y (NNI site 4), and L31V (NS5A) can all be generated via transitions (7).

Resistance is often rapidly selected against these classes of inhibitors. In contrast, resistance to NIs has been associated with single serine to threonine changes that are difficult to select; 2′-C-methylated NIs select for S282T, whereas 4′-azido-modified NIs select for S96T (11, 29). Although the specific codon for serine can vary at these positions, a change to threonine cannot

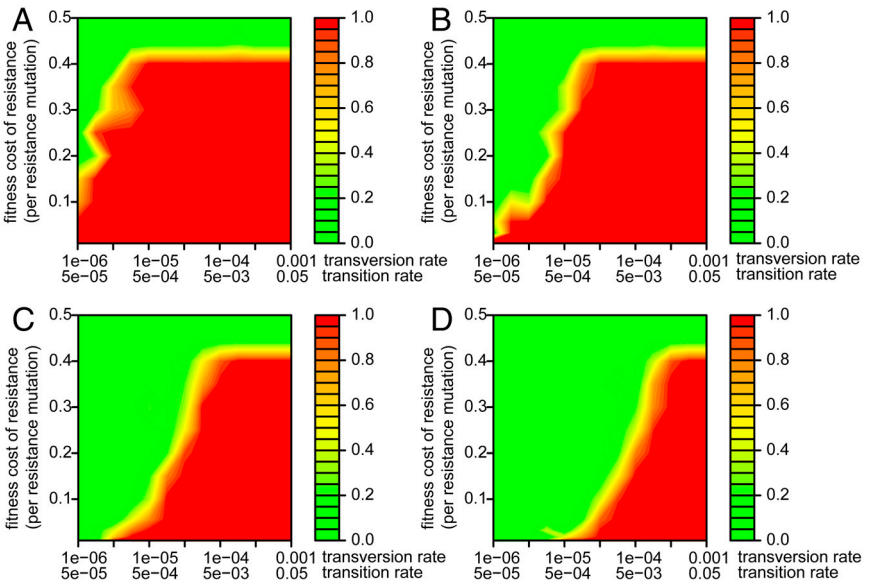

Fig. 3. Stochastic model evaluating effects of variations in fitness costs and mutation rates on the frequency of therapy failure. *A*, *B*, *C*, and *D* correspond to the frequency of therapy failure for the models in which 3 out of 3, 2 out of 3, 1 out of 3, and 0 out of 3 mutations are transitions with relatively high mutation rates. Based on our deep sequencing analysis, we assume that the mutation rate for resistance mutations involving transitions is 50 times higher than for transversions. For each parameter combination, the frequencies were determined from 100 simulations of the stochastic model described above. Green indicates that therapy is always successful (i.e., the virus population always becomes extinct), red indicates that therapy always fails (i.e., resistance mutations arise and virus population persists).

be generated through transitions. D320E in NS5A is currently the only known relevant mutation associated with resistance to the cyclophilin inhibitors, and, like S282T and S96T, D320E is difficult to select for and cannot be generated through transitions (Fig. S5 *D* and *E*) (13, 14). The high barrier to the selection of these mutations may therefore not only be explained by the diminished viral fitness of the resultant mutant variant, and/or the limited benefits conferred through low-levels of decreased drug susceptibility (30), but also by the high genetic barrier associated with the selection of transversions.

Conclusions

Collectively, the findings of this study suggest that the genetic barrier, defined as the number and nature of nucleotide changes, could be exploited in choosing potent drug combinations. Transversions, and/or multiple nucleotide changes per amino acid substitution, represent a higher genetic barrier than transitions and single nucleotide changes. Finally, we wish to point out that the selection of escape mutants from HCV-specific immune responses depends on the same principle, indicating its relevance to the development of vaccines.

Materials and Methods

Enzyme Expression and Purification. The HCV NS5B coding sequence (genotype 1b, Con1) was cloned into the expression vector pet21b (Novagen) to exclude the hydrophobic region at the C terminus of the protein (Δ21) and add a C-terminal histidine tag. Protein expression was induced in *Escherichia coli* BL21 (DE3), and NS5B purification was conducted using a combination of affinity and ion-exchange chromatography.

Pre-Steady-State Kinetics. RNA sequences used in these studies are listed in Table S1. Reaction mixtures contained 40 mM Hepes pH 8, 1 mM DTT, 15 mM NaCl, 0.5 mM EDTA, 1 μM of the required NTPs, 500 nM RNA template, and 1 μM HCV NS5B. The 5′-end labeling of 200 nM of a dinucleotide GG primer (Trilink) was carried out with [γ-^{32}P] ATP using T4 polynucleotide kinase (Invitrogen). All reactions were started with the addition of 6 mM $MgCl_2$ and allowed to proceed at room temperature for 40 min. Subsequently, nucleotides were rapidly added using a rapid quench flow apparatus (RQF, KinTek Corporation) in the presence of a heparin trap for specific time intervals and quenched with the addition of 0.5 M EDTA. Products were resolved on a 20% polyacrylamide gel and visualized using a Bio-Rad Phosphorimager.

NS3 Amplification and Deep Sequencing. All RNA isolations from plasma samples, RT-PCR amplifications, and deep sequencing were performed at Virco DBA (Virco). RNA was also isolated from 10^6 1a H77-Rluc replicon cells (31) using the RNeasy minikit (Qiagen). To reduce the contribution of errors introduced during the reverse transcription step, we utilized the high fidelity AccuScript RT (Stratagene) (23). The NS3 protease region was amplified as two overlapping amplicons using genotype specific barcoded primers. Barcoded amplicons were pooled equimolarly and sequenced on the GS-FLX instrument according to the manufacturer's amplicon sequencing protocol (454 Life Sciences). Plasmid controls encoding 1a and 1b HCV were PCR amplified and processed via deep sequencing in parallel with patient-derived HCV samples to account for the assay-derived background. To analyze sequencing data generated using the 454/Roche sequencing technology, we employed algorithms to exclude sequence reads with low quality scores, homopolymer-related errors, or characteristics of primer–dimer formation.

ACKNOWLEDGMENTS. The authors thank Viktor von Wyl for fruitful discussions. This study was supported by grants from the Cancer Research Society and the Canadian Institutes of Health Research (to M.G.). M.G. is the recipient of a career award from the Fonds de la recherche en santé du Québec. M.H.P. and R.A.K. are recipients of student and postdoctoral stipends, respectively, from the National Canadian Research Training Program in Hepatitis C. R.S.R. is the recipient of a Canadian Institutes of Health Research New Investigator Award.

1. Global Burden of Hepatitis C Working Group (2004) Global burden of disease (GBD) for hepatitis C. *J Clin Pharmacol* 44:20–29.
2. Kanwal F, et al. (2011) Increasing prevalence of HCC and cirrhosis in patients with chronic hepatitis C virus infection. *Gastroenterology* 140:1182–1188.e1.
3. Fried MW, et al. (2002) Peginterferon alfa-2a plus ribavirin for chronic hepatitis C virus infection. *N Engl J Med* 347:975–982.
4. Pawlotsky JM (2004) Treating hepatitis C in "difficult-to-treat" patients. *N Engl J Med* 351:422–423.
5. Bacon BR, et al. Boceprevir for previously treated chronic HCV genotype 1 infection. *N Engl J Med* 364:1207–1217.
6. Marcellin P, et al. (2011) Telaprevir is effective given every 8 or 12 hours with ribavirin and peginterferon alfa-2a or -2b to patients with chronic hepatitis C. *Gastroenterology* 140:459–468.e1.
7. Pawlotsky J-M (2011) Treatment failure and resistance with direct acting antiviral drugs against hepatitis C virus. *Hepatology* 53:1742–1751.
8. Martell M, et al. (1992) Hepatitis C virus (HCV) circulates as a population of different but closely related genomes: Quasispecies nature of HCV genome distribution. *J Virol* 66:3225–3229.
9. Pawlotsky JM (2011) Treatment failure and resistance with direct-acting antiviral drugs against hepatitis C virus. *Hepatology* 53:1742–1751.
10. Gao M, et al. (2010) Chemical genetics strategy identifies an HCV NS5A inhibitor with a potent clinical effect. *Nature* 465:96–100.
11. Migliaccio G, et al. (2003) Characterization of resistance to non-obligate chain-terminating ribonucleoside analogs that inhibit hepatitis C virus replication in vitro. *J Biol Chem* 278:49164–49170.
12. Le Pogam S, et al. (2010) No evidence of drug resistance or baseline S282T resistance mutation among GT1 and GT4 HCV infected patients on nucleoside polymerase inhibitor RG7128 and Peg-IFN/RBV combination treatment for up to 12 weeks: Interim analysis from the PROPEL study. *Hepatology* 52:701A–702A.
13. Coelmont L, et al. (2009) Debio 025, a cyclophilin binding molecule, is highly efficient in clearing hepatitis C virus (HCV) replicon-containing cells when used alone or in combination with specifically targeted antiviral therapy for HCV (STAT-C) Inhibitors. *Antimicrob Agents Chemother* 53:967–976.
14. Puyang X, et al. (2010) Mechanism of resistance of HCV replicons to structurally distinct cyclophilin inhibitors. *Antimicrob Agents Chemother* 54:1981–1987.
15. Zhong W, Uss AS, Ferrari E, Lau JY, Hong Z (2000) De novo initiation of RNA synthesis by hepatitis C virus nonstructural protein 5B polymerase. *J Virol* 74:2017–2022.
16. Dutartre H, Boretto J, Guillemot JC, Canard B (2005) A relaxed discrimination of 2′-O-methyl-GTP relative to GTP between de novo and elongative RNA synthesis by the hepatitis C RNA-dependent RNA polymerase NS5B. *J Biol Chem* 280:6359–6368.
17. Jin Z, Deval J, Johnson KA, Swinney DC (2011) Characterization of the elongation complex of dengue virus RNA polymerase: Assembly, kinetics of nucleotide incorporation, and fidelity. *J Biol Chem* 286:2067–2077.
18. Castro C, Arnold JJ, Cameron CE (2005) Incorporation fidelity of the viral RNA-dependent RNA polymerase: A kinetic, thermodynamic and structural perspective. *Virus Res* 107:141–149.
19. Zinnen S, Hsieh JC, Modrich P (1994) Misincorporation and mispaired primer extension by human immunodeficiency virus reverse transcriptase. *J Biol Chem* 269:24195–24202.
20. Drake JW (1993) Rates of spontaneous mutation among RNA viruses. *Proc Natl Acad Sci USA* 90:4171–4175.
21. Duffy S, Shackelton LA, Holmes EC (2008) Rates of evolutionary change in viruses: Patterns and determinants. *Nat Rev Genet* 9:267–276.
22. Mansky LM, Temin HM (1995) Lower in vivo mutation rate of human immunodeficiency virus type 1 than that predicted from the fidelity of purified reverse transcriptase. *J Virol* 69:5087–5094.
23. Arezi B, Hogrefe HH (2007) Escherichia coli DNA polymerase III ε subunit increases Moloney murine leukemia virus reverse transcriptase fidelity and accuracy of RT-PCR procedures. *Anal Biochem* 360:84–91.
24. Kato N, et al. (2005) Genetic variation and dynamics of hepatitis C virus replicons in long-term cell culture. *J Gen Virol* 86:645–656.
25. Fernandez J, et al. (2004) Long-term persistence of infection in chimpanzees inoculated with an infectious hepatitis C virus clone is associated with a decrease in the viral amino acid substitution rate and low levels of heterogeneity. *J Virol* 78:9782–9789.
26. McHutchison JG, et al. (2009) Telaprevir with peginterferon and ribavirin for chronic HCV genotype 1 infection. *N Engl J Med* 360:1827–1838.
27. Rong L, Dahari H, Ribeiro RM, Perelson AS (2010) Rapid emergence of protease inhibitor resistance in hepatitis C virus. *Sci Transl Med* 2:30ra32.
28. Chatel-Chaix L, Baril M, Lamarre D (2010) Hepatitis C virus NS3/4A protease inhibitors: A light at the end of the tunnel. *Viruses* 2:1752–1765.
29. Le Pogam S, et al. (2006) In vitro selected Con1 subgenomic replicons resistant to 2′-C-methyl-cytidine or to R1479 show lack of cross resistance. *Virology* 351:349–359.
30. Ali S, et al. (2008) Selected replicon variants with low-level in vitro resistance to the hepatitis C virus NS5B polymerase inhibitor PSI-6130 lack cross-resistance with R1479. *Antimicrob Agents Chemother* 52:4356–4369.
31. Robinson M, et al. (2010) Novel hepatitis C virus reporter replicon cell lines enable efficient antiviral screening against genotype 1a. *Antimicrob Agents Chemother* 54:3099–3106.